Hindawi Publishing Corporation
Mathematical Problems in Engineering
Volume 2013, Article ID 304856, 9 pages
http://dx.doi.org/10.1155/2013/304856

Research Article

Vertical Dynamic Impedance of Tapered Pile considering Compacting Effect

Wenbing Wu,[1] Guosheng Jiang,[1] Bin Dou,[1] and Chin Jian Leo[2]

[1] *Engineering Faculty, China University of Geosciences, Wuhan, Hubei 430074, China*
[2] *School of Computing, Engineering and Mathematics, University of Western Sydney, Locked Bag 1797, Penrith, Sydney, NSW 2751, Australia*

Correspondence should be addressed to Wenbing Wu; zjuwwb1126@163.com

Received 7 July 2013; Revised 12 October 2013; Accepted 20 October 2013

Academic Editor: Mohammad Younis

Based on complex stiffness transfer model, the vertical vibration of tapered pile embedded in layered soil is theoretically investigated by considering the compacting effect of the soil layer surrounding the tapered pile in the piling process. Allowing for the stratification of the surrounding soil and variable crosssection of the tapered pile, the pile-soil system is discretized into finite segments. By virtue of the complex stiffness transfer model to simulate the compacting effect, the complex stiffness of different soil segments surrounding the tapered pile is obtained. Then, substituting the complex stiffness into the vertical dynamic governing equation of tapered pile, the analytical solution of vertical dynamic impedance of tapered pile under vertical exciting force is derived by means of the Laplace technique and impedance function transfer method. Based on the presented solutions, the influence of compacting effect of surrounding soil on vertical dynamic impedance at the pile head is investigated within the low frequency range concerned in the design of dynamic foundation.

1. Introduction

The influence of compacting effect on the bearing capacity of jacked pile is always a focus problem in the field of geotechnical engineering, and many researchers have paid their attention to investigate this problem systematically from two aspects. The one is to study the development process of displacement field affected by compacting effect and the influence of soil parameters on this development process. For instance, Randolph et al. [1, 2] observed the deformation of surrounding soil caused by pile driving process. Luo et al. [3] pointed out that the compacting effect of jacked pile was closely related to the interaction of pile and soil. Lu et al. [4] further indicated that the compacting effect was actually affected by both the vertical pressure applied by pile driver and driving process of jacked pile. Lu et al. [5] obtained the variation law of soil displacements in the horizontal direction and depth direction by means of model test to simulate the piling process. Gong and Li [6] analyzed the mechanical problems of piling process in saturated soft clay and presented a systemic method to investigate the compacting effect of jacked pile. Luo et al. [7] discussed the influence of friction condition of pile and soil interface on the displacement field in piling process. The other one is to investigate the influence of compacting effect on the bearing capacity and sediment of pile. For example, Peng et al. [8] modified the existing load transfer function method by considering the nonlinear properties of soil. Zhang et al. [9] pointed out that the further consolidation of the surrounding soil may lead to larger settlement of pile foundation. As can be seen from the above research results, the compacting effect has a significant influence on the surrounding environment and bearing capacity of pile. Therefore, it is of great realistic significance to reveal the mechanism of compacting effect.

In recent years, the tapered pile has been widely used in engineering due to its good bearing capacity. Therefore, many researchers have investigated the bearing capacity by means of field tests and model tests [10, 11], theoretical research [12, 13], and numerical analysis [14]. Although the research on the bearing capacity of tapered pile has been very extensive and in-depth, the investigation on the compacting effect caused by pile driving is still insufficient, especially the influence of compacting effect on the vertical dynamic response of tapered pile. In the existing literature, there are only research results about the influence of compacting effect in pile driving process on the bearing capacity and ground heave presented by He et al. [15]. When investigating the vertical dynamic response of pile, there are three kinds of modeling methods for pile, that is, circular cross-section pile with finite length [16], pile with variable section impedance [17], and circular uniform viscoelastic pile [18]. The vertical dynamic response of tapered pile is only studied by Wu et al. [19] and Cai et al. [20] by taking into account its variable section property. For the interaction models of pile and surrounding soil, there are four main models, that is, the dynamic Winkler model [21], plane strain model [22, 23], three-dimensional continuum model not considering the radial displacement [24], and three-dimensional continuum model taking into account true three-dimensional wave effect of soil [25]. In order to consider the construction effect of pile, the complex stiffness transfer model is proposed [26, 27]. It can be seen that the research on the vertical coupling vibration of pile and soil varies broadly in complexity. However, the research on vertical dynamic response of tapered pile is still insufficient.

In light of this, in order to extend the application of tapered pile, this paper has introduced the complex stiffness transfer model [27] to simulate the radially inhomogeneous property of surrounding soil caused by compacting effect. Then, an analytical solution of vertical dynamic impedance at tapered pile head is derived. Based on this solution, the influence of compacting effect on the vertical dynamic impedance at the tapered pile head is studied in detail.

2. Mathematical Model and Assumptions

2.1. Computational Model. The problem studied in this paper is the vertical vibration of tapered pipe embedded in layered soil when the compacting effect is taken into account. The schematic of pile-soil interaction model is shown in Figure 1. $Q(t)$ represents the harmonic force acting on the pile head. The modeling process of tapered pile can be seen in [19], where $r_j = r_p + (H/m)(j-1)\tan\theta$ denotes the radius of the jth tapered pile segment. H, θ, and r_p denote the length, cone angle, and pile end radius of tapered pile, respectively. ρ_{pj}, V_{pj}, and A_{pj} represent the density, elastic longitudinal wave velocity, and cross-sectional area of the jth tapered pile segment, respectively. The thickness of the jth soil layer is denoted by l_j, and the depth of the top surface of the jth soil layer is denoted by h_j. The tapered pile segment can be assumed to be cylinder, and the properties of pile are assumed to be homogeneous within each segment when the segment length is small enough [19], but may vary from segment to segment.

As can be seen from the existing results, the pile surrounding soil is compacted in the piling process. This compaction may strengthen the shear modulus of surrounding soil or change the density of surrounding soil, which causes the radial inhomogeneity of surrounding soil of tapered pile. The specific modeling process can be shown as follows: the surrounding soil is divided into two annular zones, an outer semi-infinite undisturbed zone and an inner disturbed zone of width b. The outer zone medium is homogeneous, isotropic, and viscoelastic with frequency independent material damping. In order to consider the compacting effect, the inner zone is further divided into n thin concentric annular subzones numbered by $1, 2, \ldots, k, \ldots, n$, and the outer radius of the kth subzone within the jth soil layer is denoted by $b_{j,k}$. The soil medium of each subzone is assumed to be homogeneous. The dynamic shear interaction on the interface of the jth surrounding soil layer and tapered pile segment shaft is described by vertical shear complex stiffness $K_{j,1}$, which can be obtained by means of complex stiffness transfer model.

2.2. Underlying Assumptions. The pile-soil model is developed on the basis of the following assumptions.

(1) The tapered pile is viscoelastic and vertical with a variable circular cross-section, and the radius decreases linearly along the pile length direction. The support at the bottom of the tapered pile is viscoelastic.

(2) The surrounding soil is isotropic linear viscoelastic medium with a hysteretic-type damping regardless of the frequency, and it has a perfect contact with the tapered pile during vibration. The support at the bottom of the surrounding soil is also viscoelastic.

(3) The surrounding soil is infinite in the radial direction, and its free top surface has no normal or shear stress.

(4) The dynamic stress of surrounding soil transfers to the outer shaft of tapered pile through the complex stiffness on the contact interface of pile-soil system.

3. Governing Equations and Their Solutions

3.1. Dynamic Equation of Soil and Its Solution. The dynamic equilibrium equation of the kth subzone within the jth soil layer undergoing vertical deformation can be expressed as [22, 23]

$$r^2 \frac{\mathrm{d}^2 W_{j,k}}{\mathrm{d}r^2} + r\frac{\mathrm{d}W_{j,k}}{\mathrm{d}r} - {\beta_{j,k}}^2 r^2 W_{j,k} = 0, \tag{1}$$

where $\beta_{j,k} = i\omega / v_{sj,k}\sqrt{1 + iD_{sj,k}}$, $v_{sj,k}$ denotes the shear wave velocity of the kth subzone within the jth soil layer and satisfies the equation, $v_{sj,k} = \sqrt{G_{sj,k}/\rho_{sj,k}}$. $\rho_{sj,k}$, $G_{sj,k}$, $D_{sj,k}$, and $W_{j,k} = W_{j,k}(r)$ denote the density, shear modulus, material damping, and vertical displacement of the kth subzone within the jth soil layer, respectively. ω denotes the circular frequency which satisfies the equation, $\omega = 2\pi f$, and f is the general frequency.

The general solution of (1) can be expressed as

$$W_{j,k}(r) = A_{j,k} K_0\left(\beta_{j,k} r\right) + B_{j,k} I_0\left(\beta_{j,k} r\right), \tag{2}$$

where $I_0(\cdot)$ and $K_0(\cdot)$ denote the modified Bessel functions of order zero of the first and second kinds, respectively. $A_{j,k}$ and $B_{j,k}$ are undetermined constants which can be obtained by means of boundary conditions.

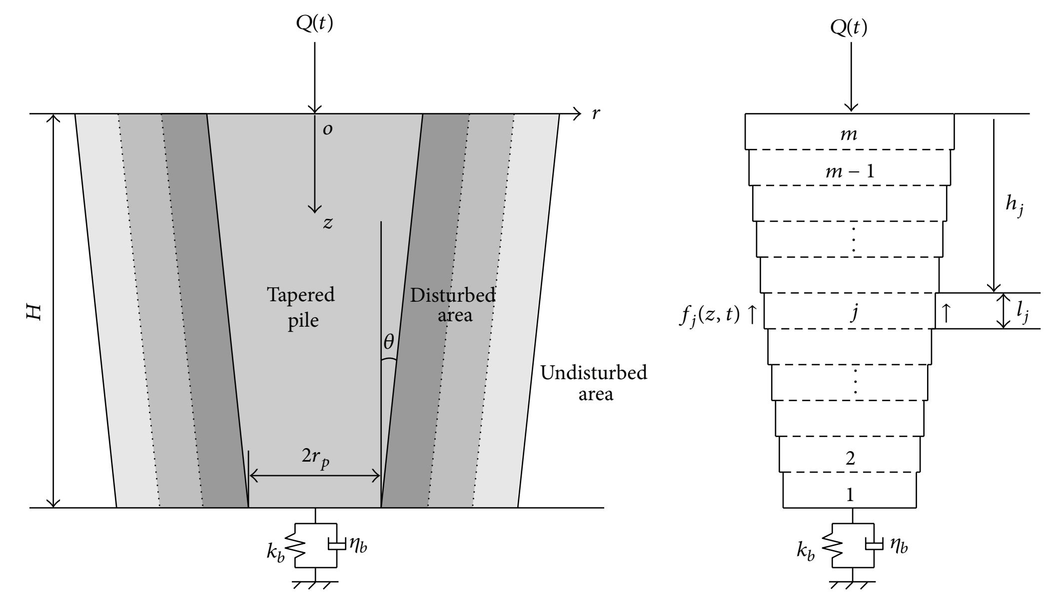

(a) Schematic of pile-soil system

(b) Schematic of pile element

FIGURE 1: Schematic of pile-soil interaction model.

(1) *Vertical Shear Complex Stiffness at the Interface of Inner-Outer Zones.* In the outer semi-infinite undisturbed zone, the vertical displacement diminishes as r approaches infinity so that $B_{n,k} = 0$. Thus, using the same method as proposed in [27], the vertical shear complex stiffness at the interface between the inner and outer zones can be derived as follows:

$$K_{j,n} = \frac{-2\pi b_{j,n}\tau_{j,n}\left(b_{j,n}\right)}{W_{j,n}\left(b_{j,n}\right)} = \frac{2\pi b_{j,n} G_{sj,n}{}^{*}\beta_{j,n} K_1\left(\beta_{j,n} b_{j,n}\right)}{K_0\left(\beta_{j,n} b_{j,n}\right)}, \tag{3}$$

where $\beta_{j,n} = i\omega / v_{sj,n}\sqrt{1 + iD_{sj,n}}$, $v_{sj,n}$ denotes the shear wave velocity of the outer semi-infinite undisturbed zone within the jth soil layer. $G_{sj,n}{}^{*} = G_{sj,n}(1 + iD_{sj,n})$. $K_1(\cdot)$ denotes the modified Bessel function of order one of the second kind.

(2) *Vertical Shear Complex Stiffness of the Inner Zones.* Since the vertical shear complex stiffness of surrounding soil is defined as the ratio of the vertical shear force to the vertical displacement at the same position, for the kth subzone within the jth inner soil layer, the vertical shear complex stiffness at the outer boundary of the kth subzone ($r = b_{j,k}$), namely, $K_{j,k}$, can be easily derived from (2) and can be expressed as

$$K_{j,k} = \frac{2\pi b_{j,k}\beta_{j,k} G^{*}_{sj,k}\left[A_{j,k} K_1\left(\beta_{j,k} b_{j,k}\right) - B_{j,k} I_1\left(\beta_{j,k} b_{j,k}\right)\right]}{A_{j,k} K_0\left(\beta_{j,k} b_{j,k}\right) + B_{j,k} I_0\left(\beta_{j,k} b_{j,k}\right)}, \tag{4}$$

where $A_{j,k}$ and $B_{j,k}$ are undetermined constants of the kth subzone within the jth inner soil layer. $I_1(\cdot)$ denotes the modified Bessel function of order one of the one kind. Then, (4) can be rewritten as follows

$$\frac{A_{j,k}}{B_{j,k}} = \frac{2\pi b_{j,k}\beta_{j,k} G^{*}_{sj,k} I_1\left(\beta_{j,k} b_{j,k}\right) + K_{j,k} I_0\left(\beta_{j,k} b_{j,k}\right)}{2\pi b_{j,k}\beta_{j,k} G^{*}_{sj,k} K_1\left(\beta_{j,k} b_{j,k}\right) - K_{j,k} K_0\left(\beta_{j,k} b_{j,k}\right)}. \tag{5}$$

In the same manner, the vertical shear complex stiffness at the outer boundary of the $(k-1)$th subzone ($r = b_{j,k-1}$) can be derived as

$$K_{j,k-1} = \frac{2\pi b_{j,k-1}\beta_{j,k} G^{*}_{sj,k}\left[A_{j,k} K_1\left(\beta_{j,k} b_{j,k-1}\right) - B_{j,k} I_1\left(\beta_{j,k} b_{j,k-1}\right)\right]}{A_{j,k} K_0\left(\beta_{j,k} b_{j,k-1}\right) + B_{j,k} I_0\left(\beta_{j,k} b_{j,k-1}\right)}. \tag{6}$$

Substituting (5) into (6), $K_{j,k-1}$ can be further rewritten as follows

$$K_{j,k-1} = \frac{2\pi b_{j,k-1}\beta_{j,k} G^{*}_{sj,k}\left[C_{j,k} K_1\left(\beta_{j,k} b_{j,k-1}\right) - D_{j,k} I_1\left(\beta_{j,k} b_{j,k-1}\right)\right]}{C_{j,k} K_0\left(\beta_{j,k} b_{j,k-1}\right) + D_{j,k} I_0\left(\beta_{j,k} b_{j,k-1}\right)}, \tag{7}$$

where

$$\begin{aligned} C_{j,k} &= 2\pi b_{j,k}\beta_{j,k} G^{*}_{sj,k} I_1\left(\beta_{j,k} b_{j,k}\right) + I_0\left(\beta_{j,k} b_{j,k}\right) K_{j,k}, \\ D_{j,k} &= 2\pi b_{j,k}\beta_{j,k} G^{*}_{sj,k} K_1\left(\beta_{j,k} b_{j,k}\right) - K_0\left(\beta_{j,k} b_{j,k}\right) K_{j,k}. \end{aligned} \tag{8}$$

By now, the recursion formula of the vertical shear complex stiffness of the inner zone has been derived in a closed form. Then, according to the stiffness of the outer zone as presented in (3) and the recursion formula (7), it is easy to obtain the vertical shear complex stiffness of the inner disturbed zones.

3.2. Dynamic Equation of Tapered Pile and Its Solution. Denoting $u_j(z,t)$ to be the vertical displacement of the jth pile segment, the frictional force of the jth soil layer acting on the surface of the jth pile segment shaft can be expressed as $f_j(z,t) = K_{j,1}u_j(z,t)$. Then, the dynamic equation of the jth pile segment can be derived as

$$E_{pj}A_{pj}\frac{\partial^2 u_j(z,t)}{\partial z^2} + A_{pj}\delta_{pj}\frac{\partial^3 u_j(z,t)}{\partial z^2 \partial t} - m_{pj}\frac{\partial^2 u_j(z,t)}{\partial t^2} - f_j(z,t) = 0, \quad (9)$$

where E_{pj}, $A_{pj} = \pi r_j^{\,2}$, m_{pj}, and δ_{pj} denote the elastic modulus, cross-section area, mass per unit length, and viscous damping of the jth pile segment, respectively.

Boundary conditions at the top and the bottom of tapered pile can be expressed as

$$\left[E_{pm}A_{pm}\frac{\partial u_m(z,t)}{\partial z} + A_{pm}\delta_{pm}\frac{\partial^2 u_m(z,t)}{\partial z \partial t}\right]\Bigg|_{z=0} = -Q(t),$$

$$\left[E_{p1}\frac{\partial u_1(z,t)}{\partial z} + \delta_{p1}\frac{\partial^2 u_1(z,t)}{\partial z \partial t} + k_b u_1(z,t) + \eta_b\frac{\partial u_1(z,t)}{\partial t}\right]\Bigg|_{z=H} = 0, \quad (10)$$

where k_b and η_b represent the distributed spring and damping coefficient in unit area at the bottom of the tapered pile, respectively. The value of k_b and η_b can be obtained using the following equations [28]

$$k_b = \frac{4\rho_{bs}V_{bs}^2 r_p}{(1-\upsilon)},$$

$$\eta_b = \frac{3.4\rho_{bs}V_{bs}r_p^2}{(1-\upsilon)}, \quad (11)$$

where ρ_{bs}, V_{bs}, υ, and r_p denote the density, shear wave velocity, Poisson's ratio, and pile end radius of tapered pile, respectively.

Continuity conditions of the interface of the adjacent tapered pile segments can be founded as

$$u_j(z,t)\big|_{z=h_j} = u_{j+1}(z,t)\big|_{z=h_j},$$

$$\left[E_{pj}A_{pj}\frac{\partial u_j(z,t)}{\partial z} + A_{pj}\delta_{pj}\frac{\partial^2 u_j(z,t)}{\partial z \partial t}\right]\Bigg|_{z=h_j} = \left[E_{p(j+1)}A_{p(j+1)}\frac{\partial u_{j+1}(z,t)}{\partial z} + A_{p(j+1)}\delta_{p(j+1)}\frac{\partial^2 u_{j+1}(z,t)}{\partial z \partial t}\right]\Bigg|_{z=h_j}. \quad (12)$$

Initial conditions of the tapered pile segments can be founded as

$$u_j(z,t)\big|_{t=0} = 0,$$

$$\frac{\partial u_j(z,t)}{\partial t}\bigg|_{t=0} = 0. \quad (13)$$

Denote $U_j(z,s) = \int_0^\infty u_j(z,t)e^{-st}\mathrm{d}t$ to be the Laplace transform of $u_j(z,t)$ with respect to t. Combining (9) with the initial conditions (13) and applying the Laplace transform yield

$${V_{pj}}^2\left(1 + \frac{\delta_{pj}}{E_{pj}}s\right)\frac{\partial^2 U_j(z,s)}{\partial^2 z} - \left(s^2 + \frac{1}{\rho_{pj}A_{pj}}K_{j,1}\right)U_j(z,s) = 0, \quad (14)$$

where V_{pj}, ρ_{pj}, and E_{pj} denote the longitudinal wave velocity, density, and elastic modulus of the jth tapered pile segment, respectively, and $E_{pj} = \rho_{pj}V_{pj}^2$. s is the Laplace transform constant which should satisfy $s = i\omega$ during the numerical analysis.

It is not difficult to obtain that the general solution of (14) which can be expressed as

$$U_j(z,s) = E_j\cos\left(\frac{\overline{\lambda}_j z}{l_j}\right) + F_j\sin\left(\frac{\overline{\lambda}_j z}{l_j}\right), \quad (15)$$

where $\overline{\lambda}_j = \sqrt{-(s^2 + K_j/\rho_{pj}A_{pj})t_j^2/(1+(\delta_{pj}/E_{pj})s)}$ is dimensionless eigenvalue. E_j and F_j are complex constants which can be obtained from boundary conditions. $t_j = l_j/V_{pj}$ denotes the propagation time of elastic longitudinal wave in the jth pile segment.

Taking into consideration the boundary conditions, the displacement impedance function at the head of the jth pile segment can be expressed as

$$Z_{pj}\big|_{z=h_j} = -\frac{\rho_{pj}A_{pj}V_{pj}\left(1+\left(\delta_{pj}/E_{pj}\right)s\right)\overline{\lambda}_j\tan\left(\overline{\lambda}_j - \varphi_j\right)}{t_j}, \quad (16)$$

where $\varphi_j = \arctan\left(Z_{p(j-1)}t_j/\rho_{pj}A_{pj}V_{pj}\overline{\lambda}_j(1+(\delta_{pj}/E_{pj})s)\right)$. $Z_{p(j-1)}$ is the displacement impedance function at the head of the $(j-1)$th pile segment, which can be obtained by virtue of the boundary conditions.

Then, following the method of recursion typically utilized in the transfer function technique [18], the displacement impedance function at the head of tapered pile can be derived as

$$Z_{pm}\big|_{z=h_m} = -\frac{\rho_{pm}A_{pm}V_{pm}\left(1+\left(\delta_{pm}/E_{pm}\right)s\right)\overline{\lambda}_m\tan\left(\overline{\lambda}_m - \varphi_m\right)}{t_m}, \quad (17)$$

where $\varphi_m = \arctan\left(Z_{p(m-1)}t_m/\rho_{pm}A_{pm}V_{pm}\overline{\lambda}_m(1+(\delta_{pm}/E_{pm})s)\right)$.

As shown in (18), the displacement impedance function can be further rewritten in terms of its real part and imaginary part which represent the dynamic stiffness and damping, respectively. And the dynamic stiffness and damping reflect the ability to resist the vertical deformation and the energy dissipation

$$Z_{pm} = K_r + iC_i. \quad (18)$$

4. Analysis of Vibration Characteristics

In order to focus on the influence of compacting effect on the dynamic response of tapered pile, the surrounding soil is set to be homogeneous in the following analysis. For practical engineering, it only needs to discretize the surrounding soil into finite layers according to the actual conditions. Parameters used here are as follows: length, density, elastic longitudinal wave velocity, pile end radius, and material damping of tapered pile are 10 m, 2500 kg/m^3, 4000 m/s, 0.3 m, and 0, respectively. As shown in [19], it is worth noting that the calculation results may be convergent if the number of the pile segment is more than $m = 200$. Therefore, in the following section, the tapered pile is divided into 200 segments with the same length.

4.1. Influence of the Number of Inner Disturbed Zone on the Vertical Dynamic Impedance at the Pile Head. Because the core idea of this paper is using the complex stiffness transfer model to simulate the radial inhomogeneity of surrounding soil caused by compacting effect, it needs to discuss the influence of the number of inner disturbed zone on the calculation results. Parameters used here are as follows. The coneangle of tapered pile is $\theta = 2^\circ$. The shear wave velocity of surrounding soil from outer undisturbed zone to inner disturbed zone increases linearly from 150 m/s to 200 m/s. The density of surrounding soil is 2000 kg/m^3 and the width of inner disturbed zone is $b = r_p$, respectively. The number of inner disturbed zone are $n = 2, 5, 10, 15, 20, 50, 100$.

Figure 2 shows the influence of the number of inner disturbed zone on the vertical dynamic impedance at the pile head. As shown in Figure 2(a), it can be observed that the dynamic stiffness increases as the frequency increases at first, but when the frequency exceeds a certain value, the dynamic stiffness may decrease with the increase of frequency. As shown in Figure 2(b), it can be noted that the dynamic damping may increase linearly with the increase of frequency when it is beyond 5 Hz. It can also be seen from Figure 2 that the computational results may be convergent when the number of inner disturbed zone is big enough for the computational curves tend to be convergent. By repeatedly calculating for different cases, all the computational results may be convergent when $n \geq 20$. Therefore, unless otherwise specified, the number of inner disturbed zone is set to be $n = 20$ in the following analysis.

4.2. Influence of the Coneangle of Tapered Pile on the Vertical Dynamic Impedance at the Pile Head. In this section, the influence of coneangle on the vertical dynamic impedance at the pile head is studied in detail by taking into account the compacting effect. Parameters used here are as follows: the shear wave velocity, density of surrounding soil, and the width of inner disturbed zone are the same as those shown in Section 4.1. The coneangle of tapered pile are $\theta = 0^\circ, 0.3^\circ, 0.5^\circ, 1^\circ, 1.5^\circ$, and 2°.

Figure 3 shows the influence of coneangle of tapered pile on the vertical dynamic impedance at the pile head within the low frequency range concerned in dynamic foundation design. As shown in Figure 3(a), the dynamic stiffness increases with the increase of frequency when the coneangle is small (i.e., $\theta \leq 1^\circ$ as shown in this example). However, when the coneangle is big enough (i.e., $\theta > 1^\circ$ as shown in this example), it can be seen that the dynamic stiffness increases with the increase of frequency at first, but the dynamic stiffness may decrease as the frequency increases when the frequency exceeds a certain value. It can also be noted that the dynamic stiffness increases as the coneangle increases at low frequencies, whereas at high frequencies the dynamic stiffness decreases with the increase of coneangle. This means that increasing the coneangle can improve the ability to resist vertical deformation of tapered pile within a certain low frequency range when other design parameters of tapered pile remain unchanged. Nevertheless, if the frequency is big enough, the ability to resist vertical deformation of tapered pile cannot be improved by simply increasing the coneangle. As shown in Figure 3(b), it can be observed that the dynamic damping may increase linearly with the increase of frequency when it is beyond 5 Hz. It can also be noted the dynamic damping increases as the coneangle increases for the same frequency, which shows that the stress wave energy propagating in the tapered pile may decay more quickly as the coneangle increases.

4.3. Influence of the Compacting Range on the Vertical Dynamic Impedance at the Pile Head. The compacting range of surrounding soil is affected by the design parameters of tapered pile, construction technology and properties of surrounding soil, and so on. So, it needs to discuss the influence of compacting range on the vertical dynamic impedance at the pile head. Parameters used here are as follows: the coneangle of tapered pile is $\theta = 2^\circ$. The shear wave velocity and density of surrounding soil are the same as those shown in Section 4.1. The width of inner disturbed zone are $b = 0, 0.5r_p, 1r_p, 1.5r_p, 2r_p$, and $2.5r_p$.

Figure 4 shows the influence of compacting range on the vertical dynamic impedance at the pile head within the low frequency range concerned in dynamic foundation design. As shown in Figure 4(a), when the compacting range is small (i.e., $b \leq 2r_p$ as shown in this example), the dynamic stiffness increases as the frequency increases within low range, whereas the dynamic stiffness deceases if the frequency is beyond a certain value. However, it can be seen that the dynamic stiffness increases with the increase of frequency when the compacting range is big enough (i.e., $b > 2r_p$ as shown in this example). It can also be seen that the dynamic stiffness increases with the increase of compacting range at low frequencies. When the frequency exceeds a certain value, the dynamic stiffness increases with the increase of the compacting range at first and then decreases as the compacting range further increases. As shown in Figure 4(b), it can be noted the dynamic damping increases as the compacting range increases for the same frequency, which means that the stress wave energy propagating in the tapered pile may decay more quickly as the compacting range increases.

In order to investigate the influence of compacting range on the vertical dynamic impedance at the pile head more detailedly, it needs to discuss the influence of compacting range changing within smaller scale on the vertical dynamic

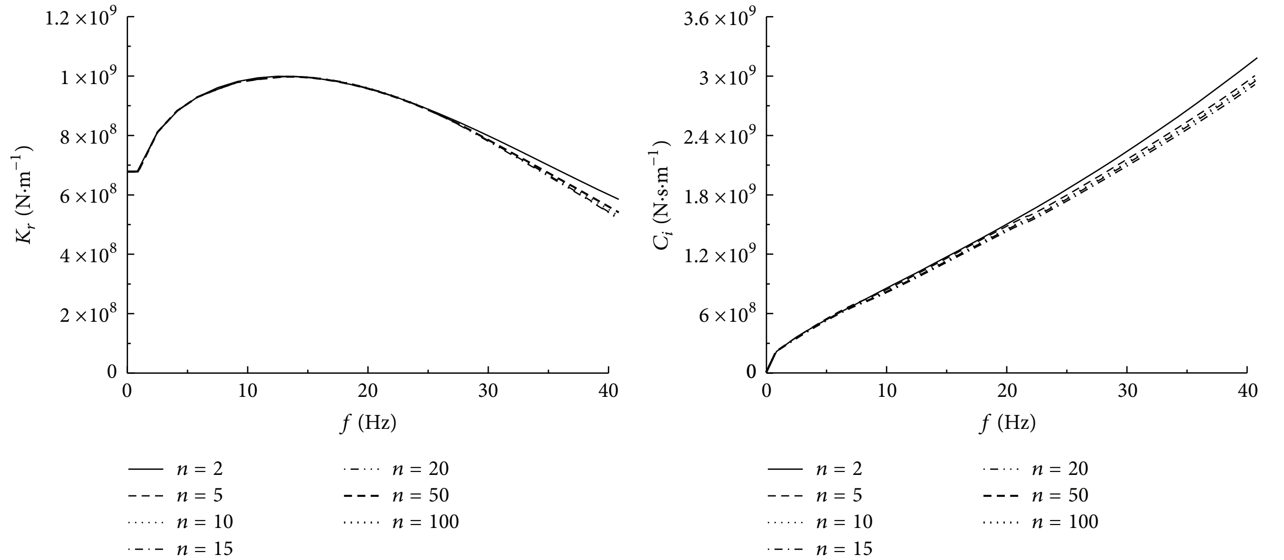

(a) Dynamic stiffness curves (b) Dynamic damping curves

Figure 2: Influence of the number of inner disturbed zone on the vertical dynamic impedance at the pile head.

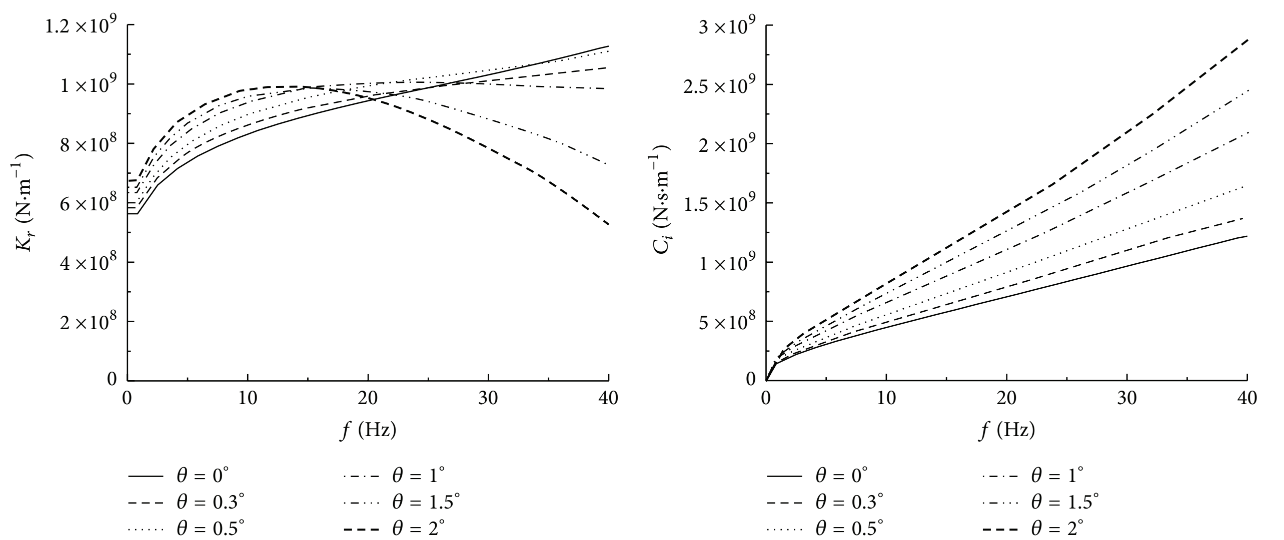

(a) Dynamic stiffness curves (b) Dynamic damping curves

Figure 3: Influence of coneangle of tapered pile on the vertical dynamic impedance at the pile head.

impedance. Parameters used here are as follows: the width of inner disturbed zone are $b = 0$, $0.05r_p$, $0.1r_p$, $0.2r_p$, $0.3r_p$, and $0.4r_p$. The other parameters are the same as those shown in the above analysis.

Figure 5 shows the influence of compacting range changing within smaller scale on the vertical dynamic impedance at the pile head within the low frequency range concerned in dynamic foundation design. As shown in Figure 5(a), it can be seen that the dynamic stiffness increases with the increase of compacting range at low frequencies, but the increase ratio is small. When the frequency is beyond a certain value, the dynamic stiffness decreases as the compacting range increases. As shown in Figure 5(b), it can be seen that the influence of compacting range changing within smaller scale on the vertical dynamic impedance is the same as that when the compacting range changes within bigger scale.

4.4. Influence of the Compacting Degree on the Vertical Dynamic Impedance at the Pile Head. Parameters used here are as follows: the coneangle of tapered pile is $\theta = 2^\circ$ and the width of inner disturbed zone is $b = r_p$. Denote shear wave velocity ratio to describe the compacting degree; that is, q represents the ratio of the shear wave velocity of inner disturbed zone to that of outer undisturbed zone. The shear wave velocity of outer undisturbed zone is 150 m/s, and the shear wave velocity ratio are $q = 1, 1.2, 1.4, 1.6, 1.8$, and 2. The other parameters are the same as those shown in Section 4.1.

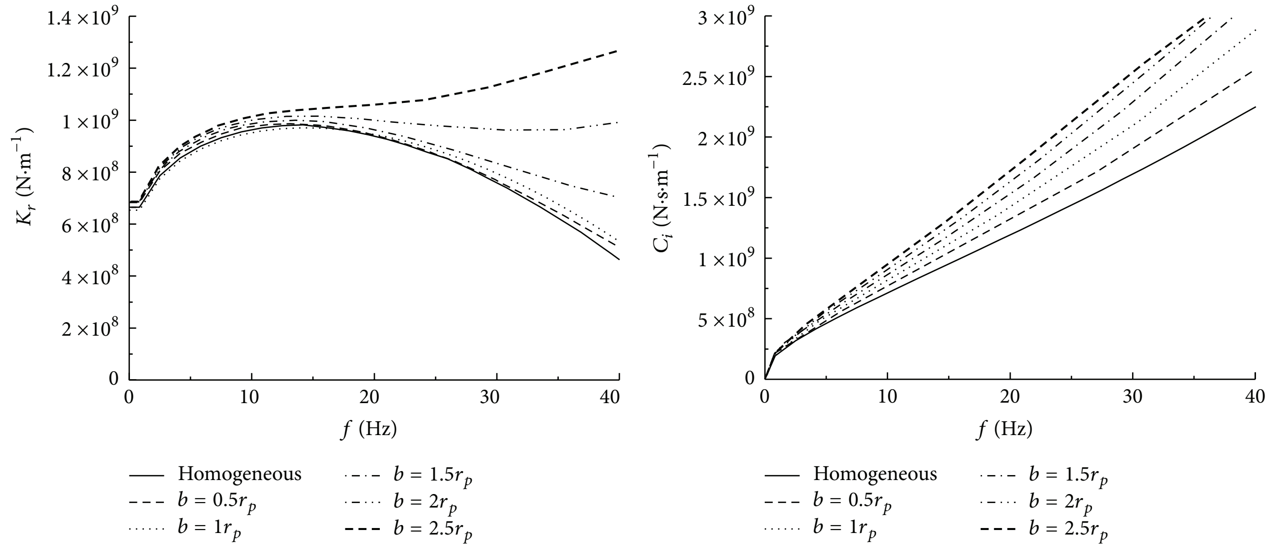

(a) Dynamic stiffness curves

(b) Dynamic damping curves

Figure 4: Influence of compacting range on the vertical dynamic impedance at the pile head.

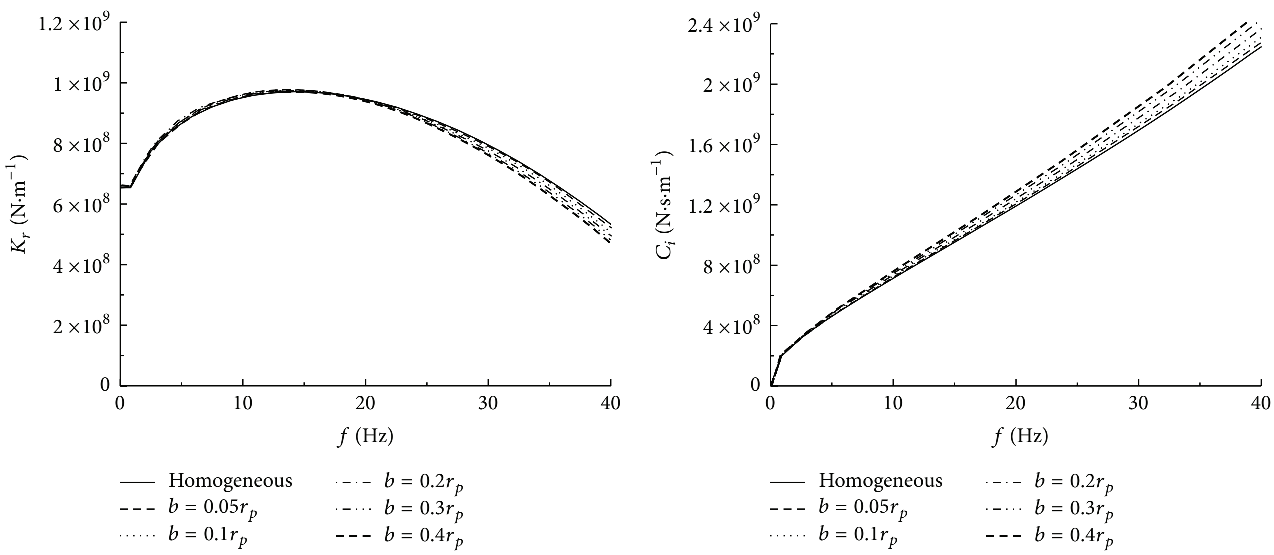

(a) Dynamic stiffness curves

(b) Dynamic damping curve

Figure 5: Influence of compacting range on the vertical dynamic impedance at the pile head.

Figure 6 shows the influence of compacting degree on the vertical dynamic impedance at the pile head within the low frequency range concerned in dynamic foundation design. As shown in Figure 6(a), it can be seen that the dynamic stiffness increases as the compacting degree increases at low frequencies, whereas at high frequencies the dynamic stiffness decreases with the increase of compacting degree. As shown in Figure 6(b), it can be seen that the dynamic damping increases as the compacting degree increases, but the increase ratio decreases as the compacting degree increases. The result shows that the stress wave energy propagating in the tapered pile may decay more quickly as the compacting degree increases.

5. Conclusions

(1) When the frequency changes within a low range, the ability to resist vertical deformation of tapered pile can be improved by increasing the coneangle of tapered pile. However, if the frequency exceeds a certain value, the ability to resist vertical deformation of tapered pile cannot be improved by simply increasing the coneangle of tapered pile. Within the low frequency range concerned in dynamic foundation design, the ability to resist vertical vibration of tapered pile can be improved by increasing the coneangle of tapered pile.

(2) When the frequency varies within a low range, increasing the compacting range of surrounding soil can

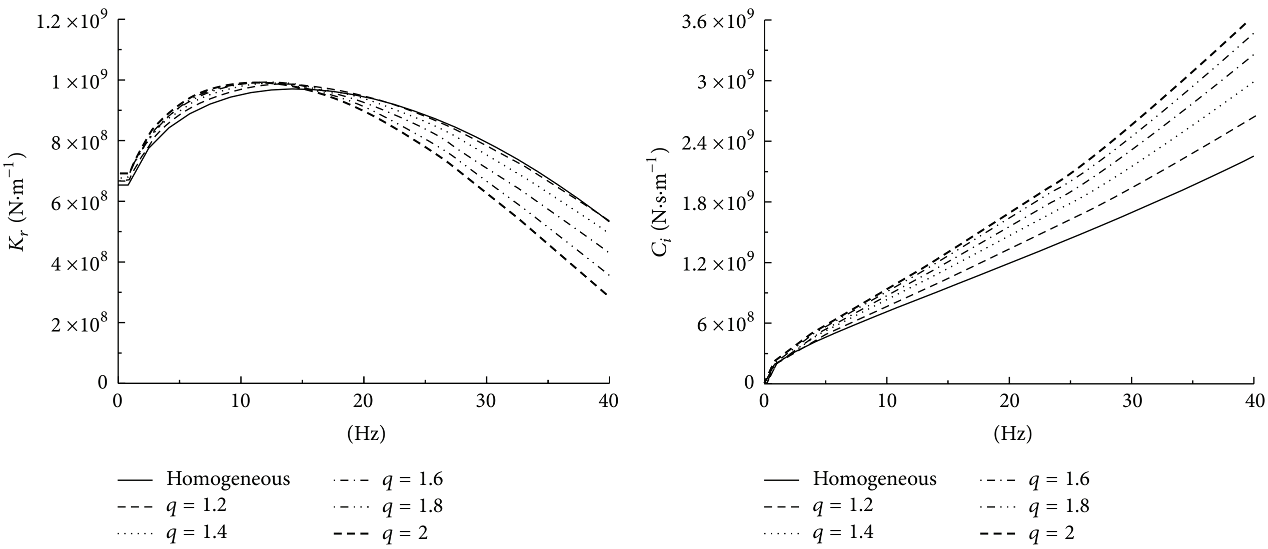

(a) Dynamic stiffness curves

(b) Dynamic damping curves

Figure 6: Influence of compacting degree on the vertical dynamic impedance at the pile head.

improve the ability to resist vertical deformation of tapered pile. However, if the frequency is beyond a certain value, increasing the compacting range within smaller scale may weaken the ability to resist vertical deformation of tapered pile, but increasing the compacting range within bigger scale may weaken the ability to resist vertical deformation of tapered pile at first and then improve the ability to resist vertical deformation of tapered pile when the compacting range is big enough. Within the low frequency range concerned in dynamic foundation design, increasing the compacting range of surrounding soil can improve the ability to resist vertical vibration.

(3) When the frequency varies within a low range, increasing the compacting degree of surrounding soil can improve the ability to resist vertical deformation of tapered pile. However, if the frequency is beyond a certain value, increasing the compacting degree of surrounding soil may weaken the ability to resist vertical deformation of tapered pile. Within the low frequency range concerned in dynamic foundation design, increasing the compacting degree of surrounding soil can improve the ability to resist vertical vibration.

Acknowledgments

This research is supported by the National Natural Science Foundation of China (Grant no. 51309207), the China Postdoctoral Science Foundation Funded Project (Grant no. 2012M521495 and no. 2013T60759), and the Fundamental Research Funds for the Central Universities (Grant no. CUG120821).

References

[1] M. F. Randolph, J. S. Steenfelt, and C. P. Worth, "The effect of pile type on design parameter for driven piles," in *Proceedings of the 7th European Conference on Soil Mechanics and Foundation in Engineering*, pp. 114–207, Brighton, UK, 1979.

[2] J. S. Steenfelt, M. F. Randolph, and C. P. Worth, "Instrumented model piles jacked into clay," in *Proceedings of the 10th International Conference on Soil Mechanics and Foundation in Engineering*, pp. 857–864, Stockholm, Sweden, 1981.

[3] Z. Y. Luo, X. N. Gong, J. L. Wang, and W. T. Wang, "Numerical simulation and factor analysis of jacked pile compacting effects," *Journal of Zhejiang University (Engineering Science)*, vol. 39, no. 7, pp. 992–996, 2005.

[4] Q. Lu, X. N. Gong, M. Ma, and J. L. Wang, "Squeezing effects of jacked pile considering static pile press machine's action," *Journal of Zhejiang University (Engineering Science)*, vol. 41, no. 7, pp. 1132–1190, 2007.

[5] J. P. Xu, J. Zhou, C. Y. Xu, and C. Y. Zhang, "Model test research on pile driving effect of squeezing against soil," *Rock and Soil Mechanics*, vol. 21, no. 3, pp. 235–238, 2000.

[6] X. N. Gong and X. H. Li, "Several mechanical problems in compacting effects of static piling in soft clay ground," *Engineering Mechanics*, vol. 17, no. 4, pp. 7–12, 2000.

[7] Z. Y. Luo, W. T. Wang, and W. Liu, "Influence analysis of friction between pile and soil on compacting effects of jacked pile," *Chinese Journal of Rock Mechanics and Engineering*, vol. 24, no. 18, pp. 3299–3304, 2005.

[8] J. Peng, J. Y. Shi, and G. Huang, "Analysis of bearing capacity of pile foundation in consideration of compaction effect," *Journal of Hohai University*, vol. 30, no. 2, pp. 105–108, 2002.

[9] X. S. Zhang, Y. M. Tiu, X. N. Gong, and J. Z. Pan, "Time-dependency analysis of soil compaction pile in soft clay ground," *Chinese Journal of Rock Mechanics and Engineering*, vol. 23, no. 19, pp. 3365–3369, 2004.

[10] J. P. Jiang and G. Y. Gao, "Comparison of belled pile, tapered pile and equal-diameter pile," *Chinese Journal of Geotechnical Engineering*, vol. 25, no. 6, pp. 764–766, 2003.

[11] J. Liu and Z. H. Wang, "Experimental study on the bearing capacity of wedge pile," *Journal of Tianjin University*, vol. 35, no. 2, pp. 257–260, 2002.

[12] M. H. El Naggar and J. Q. Wei, "Uplift behaviour of tapered piles established from model tests," *Canadian Geotechnical Journal*, vol. 37, no. 1, pp. 56–74, 2000.

[13] J. Liu, J. He, and C. Q. Min, "Contrast research of bearing behavior for composite foundation with tapered piles and cylindrical piles," *Rock and Soil Mechanics*, vol. 31, no. 7, pp. 2202–2206, 2010.

[14] W. A. Take and A. J. Walsangkar, "The elastic analysis of compressible tin-piles and pile groups," *Geotechnique*, vol. 31, no. 4, pp. 456–474, 2002.

[15] J. He, J. Liu, K. L. Chen, and C. Q. Min, "Experiment of compacting effects of static piling in clay ground with tapered pile," *Industrial Construction*, vol. 38, no. 1, pp. 74–75, 2008.

[16] K. H. Wang, K. H. Xie, and G. X. Zeng, "Analytical solution to vibration of finite length pile under exciting force and its application," *Chinese Journal of Geotechnical Engineering*, vol. 19, no. 6, pp. 27–35, 1997.

[17] K. H. Wang, K. H. Xie, and G. X. Zeng, "An analytical solution to forced vibration of foundation pile with variable section impedance and its application," *China Civil Engineering Journal*, vol. 31, no. 6, pp. 56–67, 1998.

[18] K. H. Wang, W. B. Wu, Z. Q. Zhang, and C. J. Leo, "Vertical dynamic response of an inhomogeneous viscoelastic pile," *Computers and Geotechnics*, vol. 37, no. 4, pp. 536–544, 2010.

[19] W. B. Wu, K. H. Wang, D. H. Wu, and B. N. Ma, "Study of dynamic longitudinal impedance of tapered pile considering lateral inertial effect," *Chinese Journal of Rock Mechanics and Engineering*, vol. 30, no. 2, pp. 3618–3625, 2011.

[20] Y. Y. Cai, J. Yu, C. T. Zheng, Z. B. Qi, and B. X. Song, "Analytical solution for longitudinal dynamic complex impedance of tapered pile," *Chinese Journal of Geotechnical Engineering*, vol. 33, no. 2, pp. 392–398, 2011.

[21] D. S. Kong, M. T. Luan, and Q. Yang, "Review of dynamic Winkler model applied in pile-soil interaction analyses," *World Information on Earthquake Engineering*, vol. 21, no. 1, pp. 12–17, 2005.

[22] M. Novak and F. Aboul-Ella, "Impedance functions of piles in layered media," *Journal of the Engineering Mechanical Division*, vol. 104, no. 3, pp. 643–661, 1978.

[23] M. Novak, T. Nogami, and F. Aboul-ella, "Dynamic soil reaction for plane strain case," *Journal of the Engineering Mechanical Division*, vol. 104, no. 4, pp. 953–959, 1978.

[24] C. B. Hu and T. Zhang, "Time domain torsional response of dynamically loaded pile in hysteretic type damping soil layer," *Chinese Journal of Rock Mechanics and Engineering*, vol. 25, no. 1, pp. 3190–3197, 2006.

[25] K. H. Wang, R. B. Que, and J. Z. Xia, "Theory of pile vibration considering true three-dimensional wave effect of soil and its check on the approximate theories," *Chinese Journal of Rock Mechanics and Engineering*, vol. 24, no. 8, pp. 1362–1370, 2005.

[26] M. H. El Naggar and M. Novak, "Nonlinear lateral interaction in pile dynamics," *Soil Dynamics and Earthquake Engineering*, vol. 14, no. 2, pp. 141–157, 1995.

[27] K. H. Wang, D. Y. Yang, and Z. Q. Zhang, "Study on dynamic response of pile based on complex stiffness transfer model of radial multizone plane strain," *Chinese Journal of Rock Mechanics and Engineering*, vol. 27, no. 4, pp. 825–831, 2008.

[28] J. Lysmer and F. E. Richart, "Dynamic response of footing to vertical load," *Soil Mechanical and Foundation Division*, vol. 2, no. 1, pp. 65–91, 1966.


Advances in
Operations Research
Advances in
Decision Sciences
Journal of
Applied Mathematics
Algebra
Journal of
Probability and Statistics
The Scientific
World Journal
International Journal of
Differential Equations
Hindawi
Submit your manuscripts at
http://www.hindawi.com
International Journal of
Combinatorics
Advances in
Mathematical Physics
Journal of
Complex Analysis
Journal of
Mathematics
Mathematical Problems
in Engineering
Abstract and
Applied Analysis
Discrete Dynamics in
Nature and Society
International
Journal of
Mathematics and
Mathematical
Sciences
Journal of
Discrete Mathematics
Journal of
Function Spaces
International Journal of
Stochastic Analysis
Journal of
Optimization